Design of Shock-Free Conical Nozzles

Shubham Maurya, A. Shaji, V. Mahesh, C. K. Krishnadasan, and G. Levin

Abstract Conventional conical nozzles consist of a circular-arc throat profile with tangentially attached conical section. This configuration leads to formation of a weak shock as reported in several earlier works. This article presents a method that eliminates the weak shock by incorporating slight modifications in the throat profile. The modified throat profile is analysed using method of characteristics (MOC) and validated by inviscid computational fluid dynamics (CFD) simulation.

Keywords Conical nozzle · Oblique shock · Method of characteristics · Computational fluid dynamics

1 Introduction

Conventional conical nozzles have a circular-arc throat section along with tangentially attached conical divergent section. As reported in the literature [1–4], there is formation of weak oblique shocks originating from the region just downstream of the junction of circular-arc and conical divergent section and coalescing near the axis of symmetry. Darwell and Badham [1], Migdal and Kosson [2] have analytically predicted the formation of weak oblique shocks using MOC and Back and Cuffel [3] have experimentally verified the same.

The weak oblique shock formation is due to the fact that at the junction of circular-arc and conical section the conical section acts as an obstruction to the flow which has been expanded by the circular arc [1–4]. The solution to this problem as outlined in various earlier works entails incorporation of a MOC determined transition contour between circular-arc and conical section [1, 2, 5]. This transition contour has an inflexion point.

In the present work, the oblique shocks are eliminated by introducing a *buffer* profile after circular arc. The conical divergent section is attached tangentially to this *buffer* profile. Contrary to transition contour, the *buffer* profile has no inflexion point.

S. Maurya (✉) · A. Shaji · V. Mahesh · C. K. Krishnadasan · G. Levin
Solid Propulsion and Research Entity, Vikram Sarabhai Space Centre (ISRO), Trivandrum 695022, India
e-mail: shubham.maurya3@gmail.com

P. Joshi et al. (eds.), *Advances in Engineering Design*, Lecture Notes in Mechanical Engineering, https://doi.org/10.1007/978-981-33-4684-0_4

The novelty of this study is hence the elimination of inflexion points in the design of shock-free conical nozzles.

2 Mathematical Formulation

For steady, supersonic, inviscid, irrotational and axisymmetric flow, MOC equations are given as [6]:

$$\frac{\sqrt{M^2-1}}{1+\frac{\gamma-1}{2}M^2}\frac{\mathrm{d}M}{M}+\mathrm{d}\theta-\frac{\tan\theta}{\sqrt{M^2-1}+\tan\theta}\frac{\mathrm{d}x}{r}=0 \tag{1}$$

$$\frac{\mathrm{d}r}{\mathrm{d}x}=\tan(\theta-\mu) \tag{2}$$

$$\frac{\sqrt{M^2-1}}{1+\frac{\gamma-1}{2}M^2}\frac{\mathrm{d}M}{M}-\mathrm{d}\theta-\frac{\tan\theta}{\sqrt{M^2-1}\tan\theta+1}\frac{\mathrm{d}r}{r}=0 \tag{3}$$

$$\frac{\mathrm{d}r}{\mathrm{d}x}=\tan(\theta+\mu) \tag{4}$$

where x and r are axial and radial coordinates, respectively, M is Mach number and θ is flow inclination angle (see Fig. 1). The Eqs. (1) and (2) hold along right running characteristic (C-), whereas Eqs. (3) and (4) hold along left running characteristic (C+). The above four equations are solved numerically for calculating the flow field

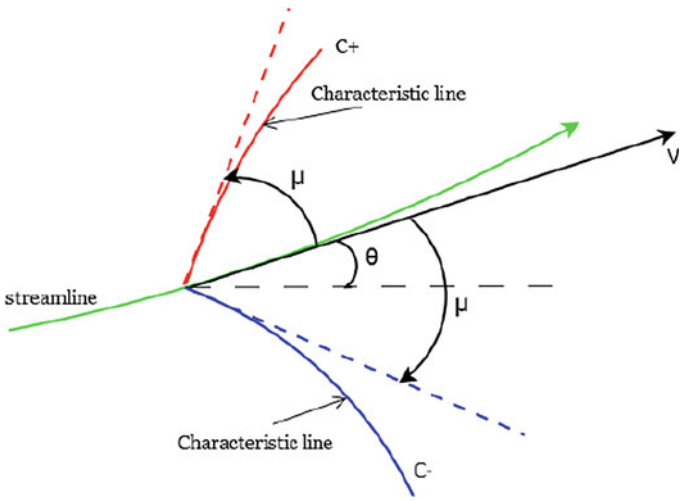

Fig. 1 Left (C+) and right (C-) running characteristic lines

parameters M and θ at locations given by coordinates x and r. The methodology for solving these equations is adopted from Ref. [6].

3 Methodology

As mentioned earlier, the conventional conical nozzles consist of a circular-arc throat section and a tangentially attached conical section (see Fig. 2). The nozzle wall angle variation along the length of nozzle (nozzle throat lies at $x = 0$) is shown in Fig. 3 (orange line). The junction of circular arc and cone can be identified from the figure as to be the point after which wall angle remains constant. It can be observed that the wall angle variation through this point is not smooth.

In the proposed shock-free nozzle design, the wall angle variation is smoothened out (see Fig. 3, blue line), resulting in a *buffer* profile as shown in Fig. 2. For the case considered, the cone half angle is chosen to be 21°. The shock-free and conventional conical nozzle geometries (with cone half angle = 21°) are plotted in Fig. 2. The *buffer* profile (blue colour, Fig. 2) increases the wall angle gradually to 21° (see Fig. 3) so that flow field computation using MOC can be worked out successfully without leading to merging of characteristics (see Fig. 4). The conical section is then attached tangentially to this *buffer* profile. The MOC computations are initiated after determining an initial-value line [7] and specifying the nozzle contour.

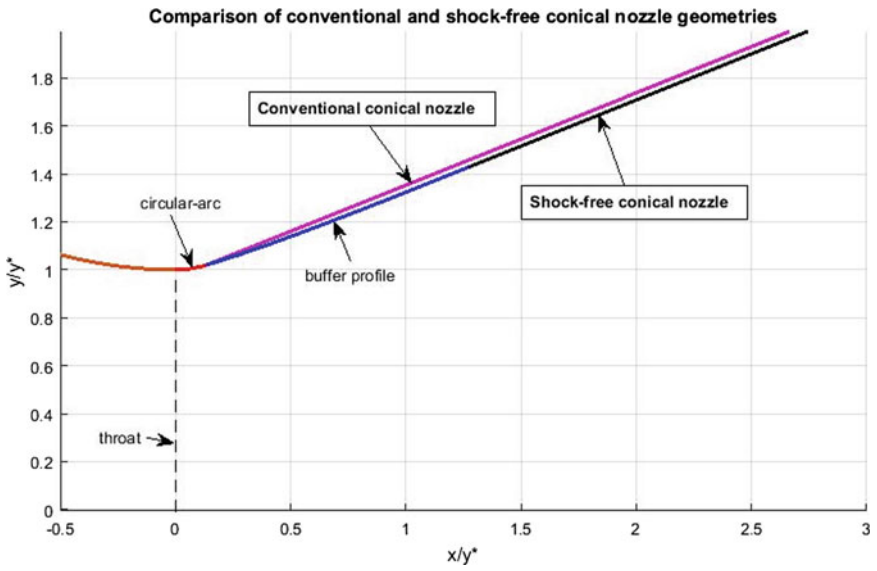

Fig. 2 Comparison of conventional and shock-free conical nozzle geometries (*Note*: y* is throat radius, and axial and radial dimensions are normalized with respect to y*)

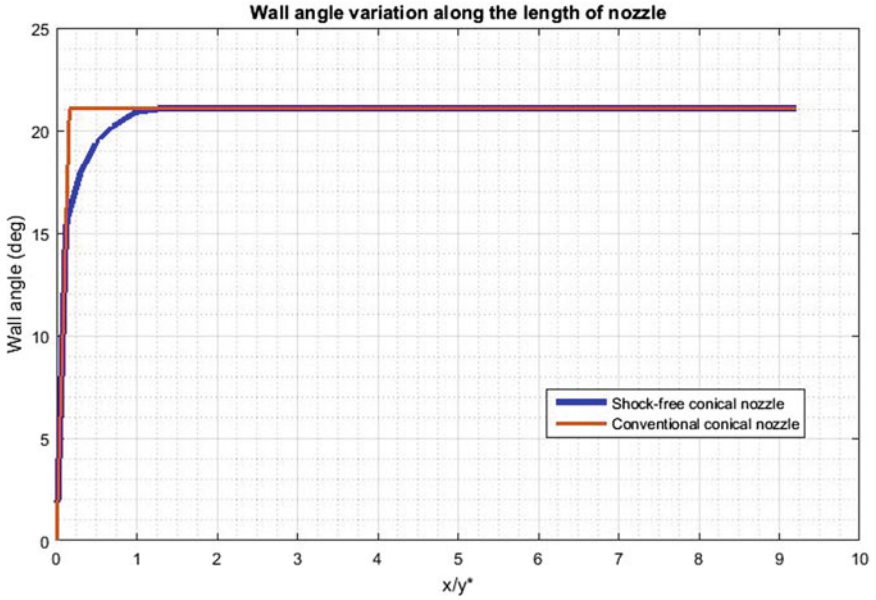

Fig. 3 Plot of wall angle variation along nozzle length for conventional and shock-free configurations

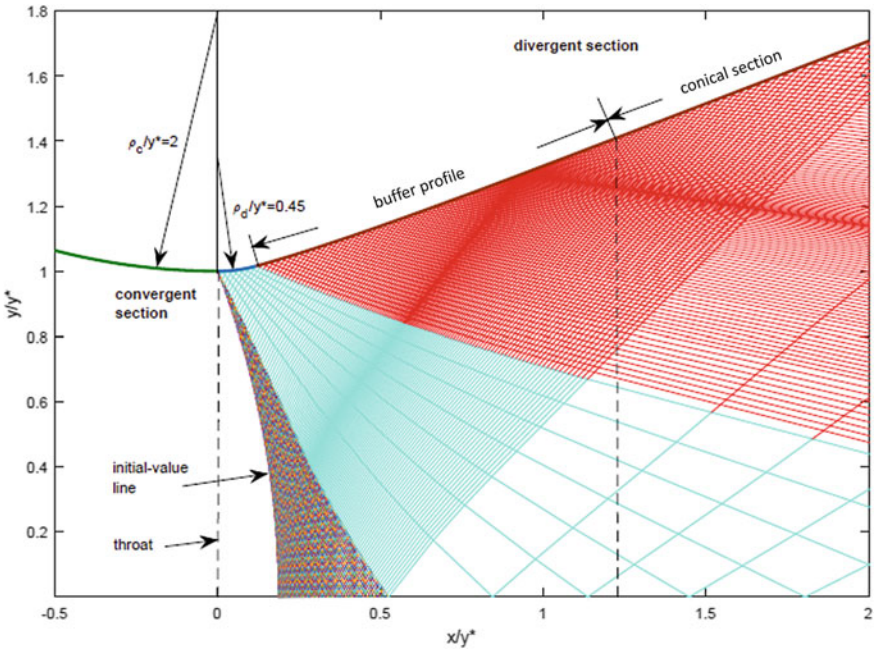

Fig. 4 Characteristic mesh inside shock-free nozzle

The selection of *buffer* profile involves trial and error as quite often the characteristics merge (indicating formation of weak oblique shock) making it impossible for the computation of rest of the flow field. Hence, the *buffer* profile is chosen in such a way that there is no coalescence or merging of characteristics so that MOC computations can be continued successfully.

4 Results and Discussion

The Mach number distribution along nozzle axis as computed using MOC is plotted in Fig. 5. It is seen that there are minor jumps in Mach number at few locations, which is arising because right running characteristics are coming closer to each other near the axis. The shock-free conical nozzle is validated using inviscid CFD simulation, and the Mach number distribution along nozzle axis is also shown in Fig. 5. The grid independency for CFD simulation was established with 18,200, 72,800 and 291,200 numbers of quadrilateral cells. The boundary conditions at nozzle inlet are specified by stagnation pressure and stagnation temperature such that the throat is

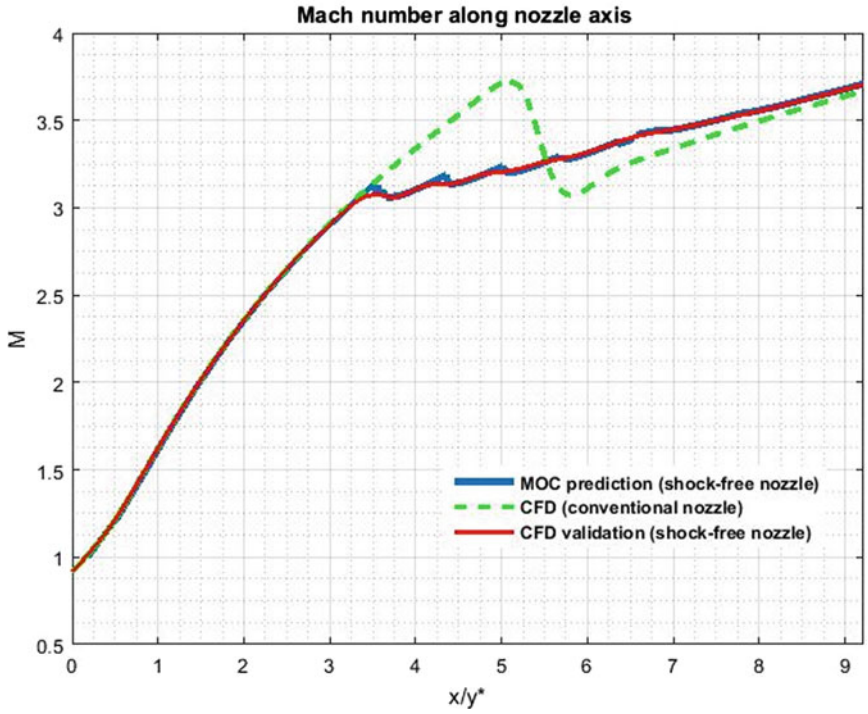

Fig. 5 Mach number variation along nozzle axis for shock-free and conventional conical nozzle configurations

choked whereas nozzle exit uses supersonic outflow boundary condition, nozzle wall is treated as adiabatic with free slip boundary condition, and nozzle axis is taken as axisymmetric. The governing equations are Euler equations, and viscosity effects are neglected. The CFD simulation was done with air exhibiting ideal gas properties and ratio of specific heats taken as 1.23 so as to validate the MOC computed flow field (since, $\gamma = 1.23$ in MOC Eqs. (1) and (3)).

Furthermore, the conventional and shock-free configurations are examined by inviscid CFD simulation. The elimination of shock in shock-free conical nozzle is confirmed through the Mach number plot along the axis of nozzle, where unlike conventional nozzle, there is no rise and fall in Mach number as observed in Fig. 5.

The Mach number palette for both conventional and shock-free conical nozzles is shown in Fig. 6, and the absence of weak oblique shock in shock-free conical nozzle is again verified.

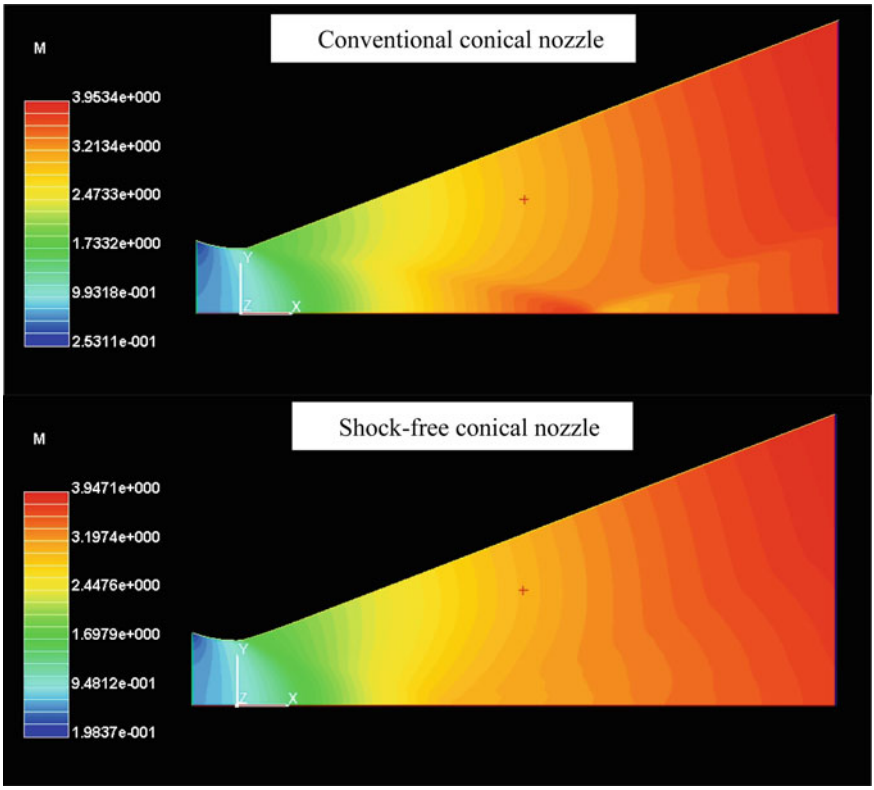

Fig. 6 Mach number palette for conventional and shock-free conical nozzle configurations. *Note* the presence/absence of a weak oblique shock in the conventional/shock-free configuration

5 Conclusions

A shock-free conical nozzle of 21° cone half angle was designed, and inside flow field was computed by MOC and validated using inviscid CFD simulation. The weak oblique shock elimination was also confirmed by inviscid CFD simulation. A major feature in this nozzle is that there is no inflexion point unlike the ones discussed in earlier works.

Further scope of this study would be to extend the shock-free conical nozzle design for other values of cone half angle. Moreover, the smoothing procedure of wall angle, i.e. selection of *buffer* profile, can be further refined so that trial and error can be avoided.

References

1. Darwell HM, Badham H (1963) Shock formation in conical nozzles. AIAA J 1(8):1932–1934
2. Migdal D, Kosson R (1965) Shock predictions in conical nozzles. AIAA J 3(8):1554–1556
3. Back LH, Cuffel RF (1966) Detection of oblique shocks in a conical nozzle with a circular-arc throat. AIAA J 4(12):2219–2221
4. Cuppoletti D, Gutmark E, Hafsteinsson H, Eriksson L-E (2014) The role of nozzle contour on supersonic jet thrust and acoustics. AIAA J 52(11):2594–2614
5. Callis LB (1966) An analysis of supersonic flow phenomena in conical nozzles by a method of characteristics. NASA TN D-3550
6. Argrow BM, Emanuel G (1988) Comparison of minimum length nozzles. J Fluids Eng 110:283–288
7. Sauer R (1947) General characteristics of the flow through nozzles at near critical speeds. NACA TM No. 1147